# Thermal Stability of Nanostructured Superhard Coatings on the Basic of TiN[1]

S.V. Ovchinnikov, A.D. Korotaev*, Yu.P. Pinzhin, A.N. Tyumentsev, V.Yu. Moshkov*, D.P. Borisov**, and V.M. Savostikov**

*Institute of Strength Physics and Material Science, 2/1, Akademichesky ave., Tomsk, 634021, Russia*
*Phone +8(3822) 53-15-69, E-mail: ovm@spti.tsu.ru*
**Tomsk State University, 36, Lenin ave., Tomsk, 634050, Russia*
***Technotron State Company, 33, Vysotsky str., Tomsk, 634040, Russia*

**Abstract – Auger electron spectroscopy, electron microscopy, X-ray structural analysis and microhardness measurements are used to study the relation between the structural phase state and mechanical properties of Ti–Si–B–N–O–C and Ti–Al–Si–N–O–C coatings in the as-deposited state and after subsequent vacuum annealing. During deposition a TiN-based phase with nanocrystalline or two-level grain structure can be formed which is distributed in the X-ray amorphous phase whose volume fraction is 20–50%. The grain structure of the coatings can be purposefully changed by alloying or deposition temperature variation. It is found that independently of the structural state and composition the coatings are superhard and have high thermal stability of superhardness and microstructure up to temperatures $T \approx 1000$ °C. The hardness reduces at $T > 1000$ °C as a result of dislocation recovery and beginning of recrystallization. The obtained results suggest that the high strength properties of the coatings are due to the presence of a dislocation substructure and high shear resistance of X-ray amorphous phases along nanocrystallite boundaries.**

## 1. Introduction

One of the key tasks in the synthesis of superhard nanostructured coatings is to provide the stability of their structure and properties in the operating temperature interval, where the upper limit can reach ~ 1000 °C. To do this, the coating structure should be designed so that to be stable to recovery, recrystallization, precipitation and roughening of phases, heterodiffusion, high-temperature creep and active loading. The line, scope of the design and its successful application depend solely on the scientifically justified interrelation between the structure and properties in a wide range of the deposition conditions.

Noteworthy in this respect is, perhaps, the only system of elements Ti–Si–N that lies at the basis of CVD-synthesized superhard coatings with *nc*-TiN/*a*-$Si_3N_4$ structure. The nature and conditions of achieving superhardness in the CVD synthesis of such coatings [1] as well as their practical application as protective coatings on cutting tools [2] have been physically justified. The thermal stability of superhardness of the Ti–Si–N-based coatings is found to result from the formation of nanosized (4–5 nm) heterophase modulated structure of spinodal decomposition at a high atomic bonding strength in the amorphous and crystalline phases.

This structure, however, sets strict requirements to the deposition conditions, i.e., temperature, nitrogen partial pressure impurity content and so on, which greatly complicates and makes more expensive the deposition technology of such coatings. That is why the application of other systems [3] and other types of structure showing high strength at elevated temperatures is demanded today.

Good candidates in this respect are multielement nanocomposites on the basis of carbon nitrides of transition metals. Now we know from the research studies with DSC, TGA, SIMS, XRD, TEM and other methods [4–10] the temperatures and activation energies of recovery, recrystallization (grain growth), residual stress relaxation, diffusion and phase transformations at annealing of these nanocomposites.

Analysis of reference data reveals, however, the necessity of more detailed study, with direct observation techniques, into local features of the defect structure, phase state and their variation micromechanisms at high-temperature annealing.

In the present paper, an attempt is made to meet the lack of this knowledge by the electron microscopic analysis of the phase composition and peculiarities of lattice bending-torsion induced by the distribution of structural defects.

Notice that the investigation is carried out for titanium nitride coatings with different concentration of alloying elements (Al, Si, B) and high (up to 10 at % in total) oxygen and carbon content. As will be shown below, such deposition conditions change the growth mechanisms of the coatings and lead to the formation of very different coating structures. In optimal deposition modes the coatings exhibit thermally stable structure and superhardness.

[1] The work was supported by the Russian Foundation for Basic Research (Grant No. 05-08-01277).

## 2. Experimental procedure

In the paper, the coatings were deposited by magnetron sputtering (system Ti–Si–B–N) and vacuum arc spraying (system Ti–Si–Al–N).

The plasma-assisted magnetron sputtering was performed by a commercial magnetron MIR-2 and a plasma source of type PINK. The coatings were sputtered of cathodes of commercial titanium VT1-0 and an SHS-produced composite cathode of a mixture of titanium, silicon and boron compounds with the following atomic percentage of the elements: Ti – 33.6%, B – 30.15%, Si – 26.25%, O – 4.8%, and C – 5.2%, at. %. The elemental composition of the coatings was varied by changing the cathode sputtering power: from 800 to 2000 W for the Ti cathode, and from 400 to 1200 W for the Ti–Si–B cathode. The cathode sputtering was carried out in a mixture of gases Ar and $N_2$ of purity 99.98 and 99.999%, respectively. The total pressure was $\approx 0.12$ Pa, nitrogen partial pressure $\approx 0.03$ Pa, the substrates temperature was 200 and 400–450 °C, and bias potential –100 V.

The vacuum arc spraying of Ti–Si–Al–N coatings was performed by a device NNV 6.6-I1 at simultaneous operation of PINK and two arc evaporators. One evaporator was made of commercial titanium VT1-0 and the second one of a hot-pressed Al–Si alloy in the ratio Al/Si = 7/3. The spraying pressure in nitrogen atmosphere was $2.66 \cdot 10^{-1}$ Pa, substrate temperature 400 °C and bias potential –200 V. The current of titanium evaporator was 80 A, Al/Si evaporator 50 A and nitrogen plasma generator 20–40 A. The aluminum and silicon content in the coatings was varied by changing the tilt angle of the specimen surface relative to the plasma stream from the Al/Si alloy evaporator.

Substrates for the both systems were made of steel 12Cr18Ni10Ti and hard alloys T15K6 and VK6 (in the Russian designation).

The produced coatings were thoroughly examined in the as-deposited state and after annealing in vacuum of $\sim 10^{-4}$ Torr. Their elemental composition was determined by Auger electron spectroscopy, structural and phase state by X-ray structural (diffractometer XRD-6000 Shimadzu) and electron microscopic analysis (microscopes EM-125 and SM-30), and by microhardness measurements (special attachment to an optical microscope Neophot 21 under load 0.2N). The thickness of the magnetron sputtered coatings after deposition was about 1 μm, and arc sprayed about 3 μm.

## 3. Results and discussion

As has been found, the above-described changing of the deposition conditions gives titanium nitride coatings with very different composition and structure. The composition of the studied coatings is given in Table 1.

The following findings have been gained in the investigation of the structural phase state of coatings with different content of alloying elements (Si, B, Al). In coatings 1 and 4, even at high diffusion mobility of adatoms (i.e., at deposition temperature 400–450 °C), a textured two-level grain structure is formed in which submicron-sized grains (up to 0.5–0.6 μm) are fragmented by low-angle (misorientation angles of up to 5°) boundaries into 20–30 nm subgrains (Fig. 1).

Table 1. Elemental composition of coatings Ti–Si–B–N (1, 2) and Ti–Al–Si–N (3, 4)

| No. coatings | Composition of coatings, at. % | | | | | | |
|---|---|---|---|---|---|---|---|
| | Ti | Si | B | Al | O | C | N |
| 1 | 46.0 | 0.4 | 0.6 | – | 7.3 | 3.0 | 43.0 |
| 2 | 39.2 | 5.0 | 6.7 | – | 5.6 | 4.7 | 38.8 |
| 3 | 36.3 | 3.6 | – | 4.3 | 4.4 | 3.2 | 48.2 |
| 4 | 47.0 | 0.2 | – | 0.8 | 5.0 | 3.0 | 43.0 |

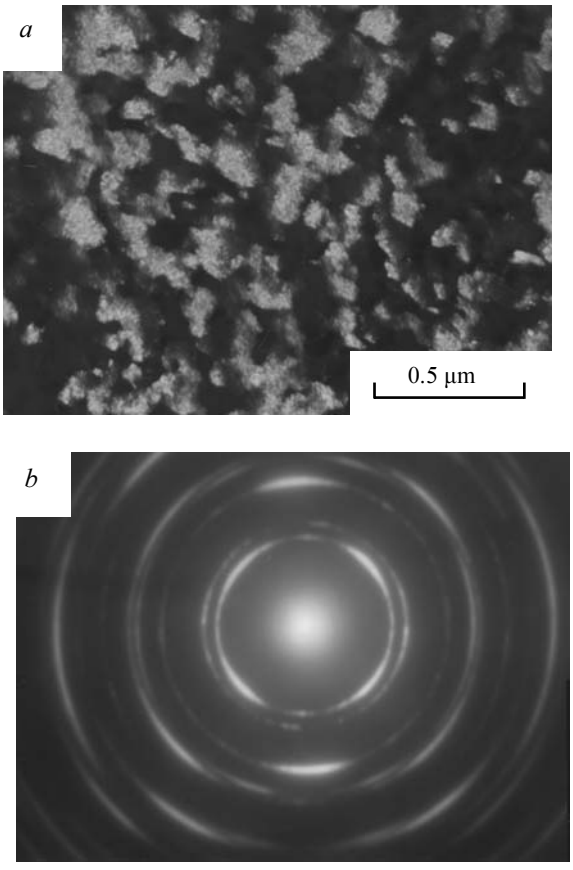


Fig. 1. Dark field image (*a*) and diffraction pattern (*b*) of the structure of Ti–Si–B–N coating 1 deposited at temperature 200 °C

The average values of curvature tensor components $\tilde{\chi}_{ij}$ calculated by extinction contour shifts as a rule reach 40 grad/μm in the grain bulk, while in near grain boundary regions they can be twice as higher. The excess density of one-sign dislocations corresponding to these curvature tensor components amounts to $5 \cdot 10^{11}$ cm$^{-2}$ (see [11] for details of the estimation technique). Besides, as reported in [12], at deposition

temperature growth to 400–450 °C the volume fraction of the two-level structure decreases, with an increase in the volume fraction of the nanocrystalline phase.

A quite unlike structure is observed in coatings with a high content of alloying elements (coatings 2 and 3). In this case, independently of the deposition temperature the coatings consist of chaotically oriented nanocrystals up to 20 nm in size (Fig. 2).

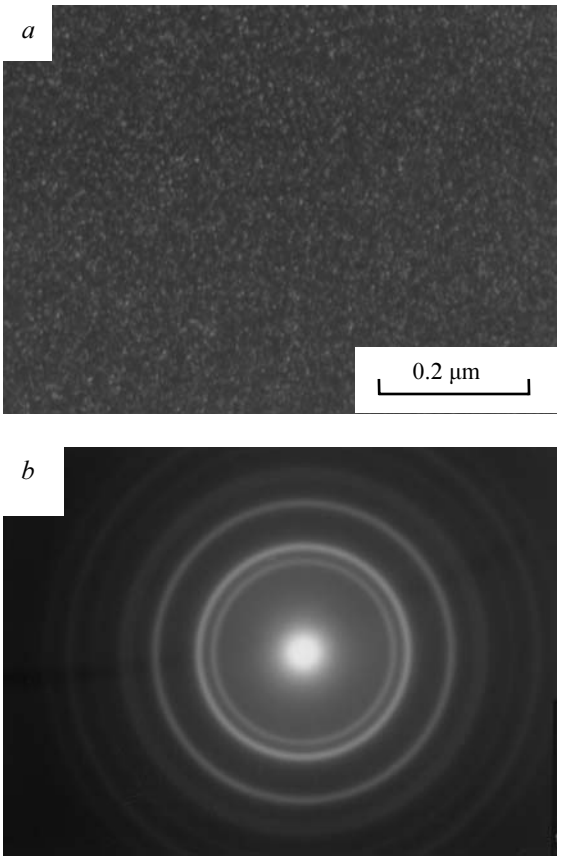


Fig. 2. Dark field image (*a*) and diffraction pattern (*b*) of the structure of Ti–Si–B–N coating 2 deposited at temperature 200 °C

According to X-ray structural analysis, the volume fraction of the X-ray amorphous structural phase increases from 20–25% in coatings 1, 4 to ~ 50% in coatings 2, 3.

The above data suggest that the content of impurities (Si, B, Al) greatly influences the structural phase state and growth mechanism of titanium nitride coatings. Particularly, with an increasing content of alloying elements, which are hardly soluble in the equilibrium conditions, to a critical value and/or to their diffusion mobility the boundaries of growing crystals are saturated with these elements and hence the grain size reduces. The given effect, along with the nonequilibrium deposition conditions, favors the formation of chaotically oriented nanocrystals.

Evidently, alloying elements in the two-level grain structure are also to a great extent dissolved at intragranular defects (subboundaries), stabilizing the position of the defects but not impeding the grain growth. It is found that the nucleation texture in this structure changes for growth texture, the grain size increases with coating thickness and residual stresses arise, especially close to grain boundaries [12]. All the characteristics as well as fracture surfaces of the coatings are indicative of their columnar growth mechanism.

The microhardness measurements show that in optimal deposition conditions the hardness of the considered coatings with different structure exceeds 40 GPa, i.e., the coatings are superhard (Table 2).

Table 2. Microhardness of coatings Ti–Si–B–N (1, 2) and Ti–Al–Si–N (3, 4) in the as-deposited state

| No. coatings | Temperature of substrate, °C | Average value of microhardness, $H_\mu$, GPa |
|---|---|---|
| 1 | 200 | 43–46 |
| | 400–450 | 50–55 |
| 2 | 200 | 33–35 |
| | 400–450 | 50–52 |
| 3 | 400 | 44.3 |
| 4 | 400 | 47.1 |

The investigation findings on the thermal stability of the both coating systems are qualitatively similar. They will be illustrated by the example of Ti–Si–B–N coatings with the two-level structure (low-temperature coating 1) and nanocrystalline structure (high-temperature coating 2). The hardness variation in these coatings vs. annealing temperature is given in Table 3.

Table 3. Hardness of Ti–Si–B–N coatings vs. vacuum annealing temperature

| Temperature of annealing, °C | 400 | 600 | 800 | 900 | 1000 | 1100 |
|---|---|---|---|---|---|---|
| $H_\mu$, GPa (coating No. 1) | 42 | 41 | 37 | 38 | 36 | 31 |
| $H_\mu$, GPa (coating No. 2) | 59 | 53 | 52 | 52 | 49 | 23 |

The obtained results are interesting in a few respects.

First, the hardness of the coatings with a high content of alloying elements is found to grow by 10–15% at low-temperature annealing. Such a “self-hardening” effect was noticed earlier in [1, 4] where it is related to the completion of phase decomposition and formation of amorphous grain boundary layers of optimal thickness. In our case, the hardness growth occurs together with crystal size reduction from 10 to 5 nm, which agrees with the general knowledge about the grain size/hardness correlation under inhibited grain boundary sliding. However, special analysis techniques are needed to understand the above structural transformation mechanism, which is the subject of our further research.

Second, the coatings preserve high hardness and superhardness up to annealing temperature 1000 °C inclusive. No visible changes in the coating structure and phase composition are therewith observed. The considered experimental data suggest that the superhardness of the studied coatings is not related to long-range internal stresses. The stress relaxation, according to [7, 13], in TiN coatings occurs at annealing temperatures $T \le 700$ °C. In carbon- [5] or aluminum-alloyed [14] TiN coatings the internal stresses relax at $T < 900$ °C. Their sources in these coatings are point defects [5, 7, 14]. The diffusion of nitrogen atoms activated by these defects with activation energy 2.0÷2.5 eV takes place at $T < 600$ °C, while that of titanium atoms with energy about 3.5 eV occurs at $T \le 900$ °C. The obtained results thus indicate that the diffusion processes occurring at $T < 1000$ °C in the nanograin bulk do not control changes in the defect substructure on which the coating hardness depends. Besides, by the data of X-ray structural analysis, they are also not enough for the crystallization of X-ray amorphous phases, at least at temperature 900 °C.

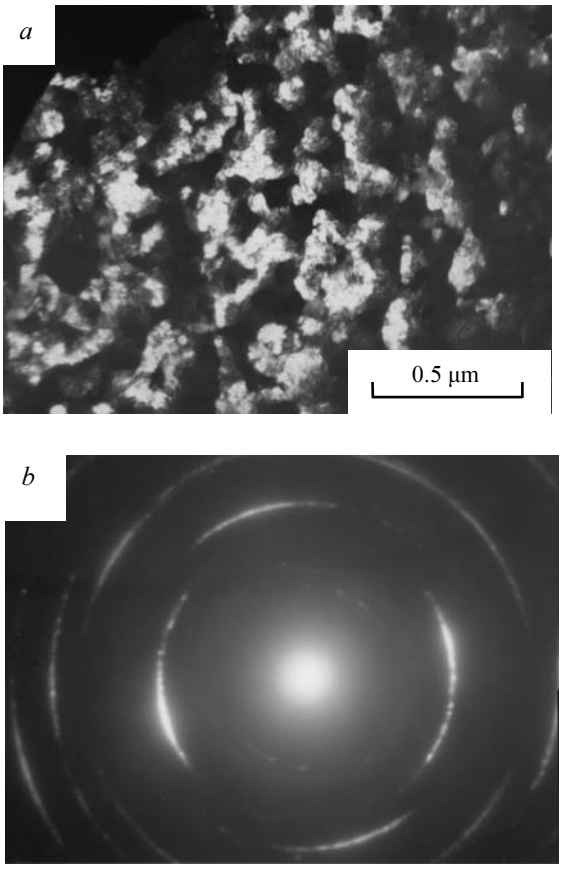


Fig. 3. Dark field image (*a*) and diffraction pattern (*b*) of the structure of Ti–Si–B–N coating 1 deposited at temperature 200 °C and then annealed at 1100 °C in vacuum

Third, the hardness reduction observed at annealing temperature 1100 °C is accompanied by significant changes in the structural phase state of the studied coatings. In this case, coatings with the two-level structure (Fig. 3) demonstrate dislocation recovery with dislocation density decrease by 25–30%, respective subgrain size growth and precipitation of second phases ($Ti_2N$ nitride with reduced content of nitrogen and titanium oxides).

Obviously, these changes lead to hardness reduction. It is also possible that the formation of the nitride with reduced nitrogen content is preceded by nitrogen impoverishment of the TiN lattice. A consequence of that can be a decrease in its lattice parameter to ~ 0.42 nm as compared to the tabulated data, which was revealed experimentally in the calculation of electron diffraction patterns. The concurrent formation of non-stoichiometric TiN nitride should also reduce hardness [15].

For the nanocrystalline structure, annealing at 1100 °C results in grain growth from 10 to 25–80 nm, which is accompanied by the precipitation of nanosized titanium oxide and silicide particles (Fig. 4).

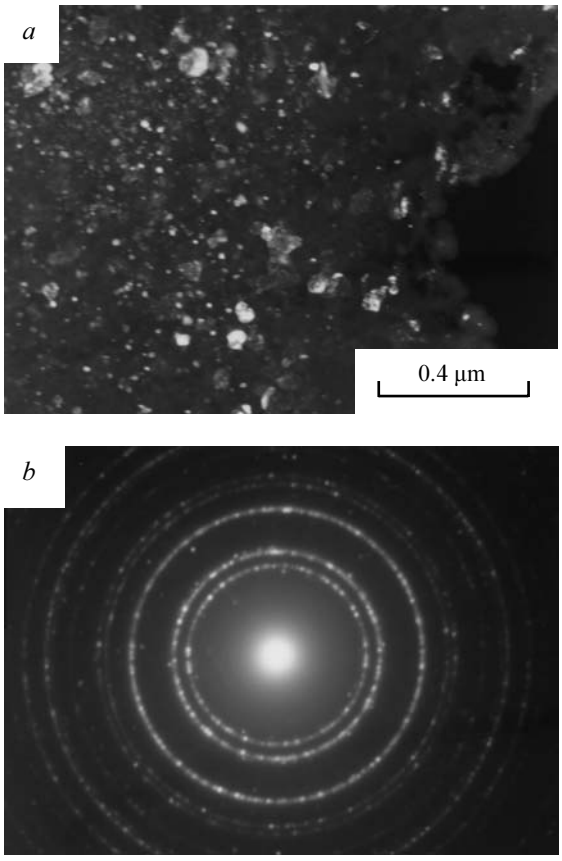


Fig. 4. Dark field image (*a*) and diffraction pattern (*b*) of the structure of Ti–Si–B–N coating 2 deposited at temperature 400 °C and then annealed at 1100 °C in vacuum

In this case, there is a correlation between the growth rates of the grain size, TiN lattice parameter and volume fraction of second-phase particles. Particularly, after such annealing the rate of structural

phase transformations is different in different regions; in the zones with a large amount of precipitated second-phase particles the TiN lattice parameter and its grain size are the largest.

Second, for the coatings with high content of alloying elements the hardness reduction at the given annealing temperature is much more pronounced than for coatings with the two-level structure. This means that for the former the governing factor in the generation of thermally stable superhard state is the high volume fraction of grain boundary X-ray amorphous phases. While for the latter it is the high level of substructural hardening associated with extremely small (10–20 nm) size of the coating subgrains.

## 4. Conclusions

Based on the above findings the following conclusions can be made:

1. In coatings of systems Ti–Si–B–O–C–N and Ti–Al–Si–O–C–N a TiN-based phase with nanocrystalline or two-level grain structure can be formed which is distributed in the X-ray amorphous phase of volume fraction 20–50%. The grain structure pattern and growth mechanism of the coatings can be purposefully changed by alloying or deposition temperature variation.

2. Independently of the structural state and composition, the coatings are superhard and have high thermal stability of superhardness and microstructure up to temperatures $T \approx 1000$ °C. The hardness reduction is observed at $T > 1000$ °C as a result of dislocation recovery and beginning of recrystallization.

3. We suppose that the high strength properties of the coatings are due to the presence of a dislocation substructure and high shear resistance of X-ray amorphous phases along the nanocrystallite boundaries of the TiN-based phase.

## References


[1] S. Veprek, M.G.-J. Veprek-Heiman, P. Karvankova, and J. Prochazka, Thin Solid Films **476**, 1 (2005).

[2] R.A. Andrievskii, Functional materals **4**, 8 (2007).

[3] A. Raveh, I. Zukerman, R. Shneck, R. Avni, and I. Fried, Surface and Coating Technol. **201**, 6136 (2007).

[4] H.-D. Männling, D.S. Patil, K. Moto, M. Jilek, and S. Veprek, Surface and Coating Technol. **143**–**147**, 263 (2001).

[5] L. Karlsson, A. Hörling, M.P. Johansson, L. Hultman, and G. Ramanath, Acta Materialia **50**, 5103 (2002).

[6] C. Mitterer, P.H. Mayrhofer, and J. Musil, Vacuum **71**, 279 (2003).

[7] L. Hultman, Vacuum **57**, 1 (2000).

[8] P.H. Mayrhofer, and M. Stoiber, Surface and Coating Technol. **201**, 6148 (2007).

[9] Ph.V. Kiryukhantsev-Korneev, D.V. Shtansky, M.I. Petrzhik, E.A. Levashov, and B.N. Mavrin, Surface and Coating Technol. **201**, 6143 (2007).

[10] H. Willmann, P.H. Mayrhofer, P.O.Å. Persson, A.E. Reiter, L. Hultman, and C. Mitterer, Scripta Materialia **54**, 1847 (2006).

[11] A.D. Korotaev, A.N. Tyumentsev and V.F. Sukhovarov, *Dispersion hardening of refractory metals*, Novosibirsk, Nauka, 1989, p. 211.

[12] A.D. Korotaev, D.P. Borisov, V.Yu. Moshkov, S.V. Ovchinnikov, K.V. Oskomov, Yu.P. Pinzhin, V.M. Savostikov, and A.N. Tymentsev, Izv. Vyssh. Uchebn. Zaved. Fiz. **7**, 3 (2007).

[13] P.H. Mayrhofer, F. Kunc, J. Musil, and C. Mitterer, Thin Solid Films **415**, 151 (2002).

[14] A. Hörling, L. Hultman, M. Oden, J. Cjölen, and L. Karlsson, Surface and Coating Technol. **191**, 384 (2005).

[15] H.J. Goldschmidt, *Interstitial alloys*, Moscow, Mir, 1971, p. 424.